Supplementary Information

Improved utilization of biomass-derived carbon by co-processing with hydrogen-rich feedstocks in millisecond reactors

Joshua L. Colby, Paul J. Dauenhauer, Brian C. Michael, Aditya Bhan and Lanny D. Schmidt

The supplementary material is organized into the following sections:

1) Supporting Information: Experimental Methods

The reactor setup and operation, effluent characterization, and catalyst preparation methodology are described in this section. Further experimental details for similar systems can also be found elsewhere.[1,2]

Reactor Setup

Experiments were performed in a 20 mm I.D., 22 mm O.D. vertical quartz reactor tube. A 17 mm O.D., 10 mm deep α-Al_2O_3 foam was used to support a 60 mm bed of 1.3 mm diameter catalyst spheres. The ceramic foam was inserted through the bottom of the reactor tube and held in place via friction fit against the quartz wall using ceramic cloth. The catalyst spheres were then charged from the open top of the quartz tube, before sealing the reactor for use.

Temperatures were measured at 20 mm and 40 mm from the front (top) face of the catalyst by 0.25 mm O.D. type K thermocouples. The thermocouples were inserted from the bottom of the reactor tube while loading the foam catalyst support, and held in place via friction fit between the quartz wall and ceramic cloth. The thermocouples were bent at an angle to place their tips at the middle of reactor tube and desired depth prior to catalyst loading.

Cellulose feed was controlled using a custom laboratory scale auger/hopper system. A 0.25 in. auger functioned as a volumetric feeder, moving cellulose from a sealed acrylic hopper to the reactor at constant rates. The auger was controlled by a laboratory mixer accurate to ±1 RPM, allowing for accurate control of cellulose mass feed rate. Lattice NT 200 microcrystalline cellulose purchased from FMC Biopolymer was used for these experiments. The cellulose was sieved to eliminate particles <300 μm to prevent small particles from adhering to the reactor wall before reaching the catalyst and to ensure uniform flow rates by facilitating flow into the auger. The cellulose was mixed with feed gases before entering the quartz tube for reaction.

N_2, O_2, CH_4, and CO_2 gas flow rates were controlled using mass flow controllers operated by LabVIEW software, accurate to ±0.05 SLPM. Feed gases were fed through the hopper prior to being mixed with the cellulose and entering the reactor to equilibrate the gas mixture within the hopper to the desired feed concentration.

Reactor Operation

The reactor was started by first flowing a fuel-rich mixture of methane and oxygen diluted in nitrogen through the catalyst bed. An isolated portion of the catalyst was then heated by applying a butane torch flame to the exterior of the quartz reactor tube. Once the isolated portion of the catalyst reached ~300 °C the autothermal partial oxidation of the methane was initiated raising the entire bed temperature to ~900 °C. Insulation was then added to the exterior of the quartz reactor tube to minimize heat loss to the surroundings. Once the catalyst bed temperature reached steady state, cellulose was added at the desired flow rate. After the cellulose flow rate reached steady state the CH_4, O_2, N_2, and CO_2 flow rates were set to their desired values.

Gravimetric measurements were taken prior to reactor assembly to determine cellulose flow rate as a function of auger turn rate.

Measurement

Effluents were quantified and identified using an HP 5890 gas chromatograph (GC) equipped with a Plot Q capillary column and a thermal conductivity detector, which was calibrated to detect permanent gases and higher hydrocarbon species. Gas samples (0.5 mL) were taken with a syringe through a sampling port downstream of the catalyst bed and injected into the GC. Products were quantified using predetermined response factors (using nitrogen as the internal standard) found using known quantities of premixed gases. Products were identified based upon their retention time in the column. Balances for H, O, and C generally closed within 5%.

A N_2 gas stream was added downstream of the catalyst bed and upstream of the sampling port to provide an internal standard for experiments with no N_2 in the gas feed. This was only necessary for experiments with feed gas ratios $CO_2/O_2>3.5$ and $N_2/O_2=0$. Under these conditions the CO_2 concentration in the effluent was very high causing increased variance in the carbon balances, requiring closure of the carbon balance around CO_2. All experiments were repeated at least three times, usually over multiple catalyst beds with no observable differences.

Catalyst Formulations

Catalysts used in these experiments were prepared on Saint-Gobain NorPro Corporation 1.3 mm diameter α-Al_2O_3 spheres, details for which can be found elsewhere.[2] A 5 wt% γ-Al_2O_3 washcoat was deposited on the α-Al_2O_3 spheres using the incipient wetness technique, which likely increases surface area and stabilizes the catalyst.[3] Once dry, the spheres were calcined in stagnant air for 6 hrs at 600 °C. The process was then repeated to add 1 wt% Rh and 1 wt% Ce catalyst to the γ-Al_2O_3 using a solution of $Rh(NO_3)_3$ and $Ce(NO_3)_3 \cdot 6H_2O$ in distilled water. The catalysts were run under representative operating conditions in the reactor for at least 1 hr prior to data acquisition, and all catalysts were used for >25 hrs with no observable deactivation.

2) Supporting Information: Construction of Figure 3

The numbers recorded/reported in Figure 3 (also Figure S4) required adiabatic equilibrium information for the CPO of cellulose and CH_4 at four constant feed ratios in air with no preheat, varying the ratios Air/Fuel and Air/CO_2 over all possible concentrations. The results are presented as a ternary diagram with each axis representing a different reactor feed. The process of calculating the adiabatic equilibrium information and assembling the figure is described in this section.

Adiabatic Equilibrium Calculations

A large number of equilibrium calculations (on the order of tens of thousands) were required for the assembly of Figure 3. To allow for efficient acquisition of the desired data, a program was written in Python programming language and interfaced with Cantera, an open source equilibrium solver developed by Prof. David Goodwin at Caltech. Cantera calculates the thermodynamic equilibrium of a system, in this case a two phase system, by using the method of element potential.

Cantera was used to calculate isothermal equilibrium concentrations for specified feed conditions holding preheat constant at 25 °C and pressure constant at 1 atm. Species included in the calculation were H_2, H_2O, CO, CO_2, N_2, O_2, CH_4, and a variety of higher hydrocarbons in the gas phase, and graphite in the solid phase. Results were used to calculate total heat capacity of the system and heat of reaction (using information available through the NIST Chemistry WebBook). The heat of formation of cellulose was obtained from Milosavljevic et al who determined it to be -1020.1 kJ/equiv "where '1 equiv' of cellulose corresponds to 1 formula weight equivalent of 162 g per cellulose repeat unit."[4] The bisection method was used to converge to the adiabatic equilibrium condition for each feed composition by determining the temperature at which the sum of all species heat capacities balanced with the heat of reaction.

To verify the results obtained using Cantera, equilibrium calculations were also performed for selected data points using HSC Chemistry software (commercially available), which calculates equilibrium by minimizing Gibbs free energy of formation for the system.[5] In addition to graphitic carbon, amorphous carbon was included in the solid phase for equilibrium calculations performed with HSC Chemistry software.

Compilation of Figure 2 in the Manuscript

Adiabatic equilibrium information was determined for approximately 10,000 equally spaced points covering the entire ternary diagram of Figure 2, which displays all possible feed ratios for the fuel, air, and CO_2 mixture. Data in Figures S1, S2, and S3 are not equally spaced because data has been renormalized to exclude N_2. We assumed 100% conversion of cellulose for all calculations, consistent with experimentally observed behavior.

Results were first analyzed to determine operating conditions where there was zero net generation of carbon dioxide, meaning there is no more CO_2 in the effluent of the reactor than in the feed. This region was determined by analyzing the carbon selectivity to CO_2, where carbon selectivity to CO_2 was defined as:

$$S_{CO_2} = \frac{n_{CO_2,equil} - n_{CO_2,feed}}{n_{C,feed} - n_{CO_2,feed}} \tag{ES1}$$

where S_{CO_2} is the carbon selectivity to CO_2, $n_{CO_2,equil}$ is the number of moles of CO_2 at adiabatic equilibrium, $n_{CO_2,feed}$ is the number of moles of CO_2 in the feed, and $n_{C,feed}$ is the total number of moles of carbon in the feed (equal to the total number of moles of carbon in the effluent). As an example, all points where the selectivity to CO_2 is a negative value for $C_{Cellulose}/C_{CH4}=0.25$ are presented in Figure S1.
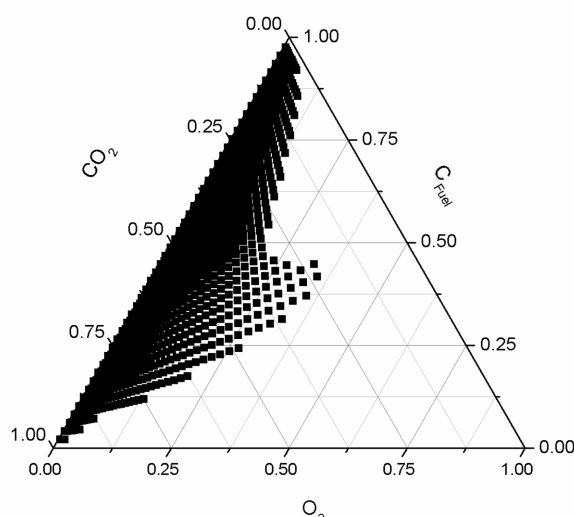

Figure S1: Adiabatic equilibrium calculations for CPO of cellulose and CH_4 at $C_{Cellulose}/C_{CH4}=0.25$ in air with no preheat and varying ratios of Air/Fuel and Air/CO_2 over all possible concentrations. Results (renormalized without nitrogen) describe a regime where the selectivity to CO_2 is less than zero, meaning there is less CO_2 in the effluent than in the feed. The boundary of this region represents operating conditions where there is zero net carbon dioxide generated, meaning the effluent contains the same amount of CO_2 as the feed.

In CPO reactors it is important to operate under conditions free of stable solid carbon formation for two reasons: 1) carbon is an undesired product, and 2) carbon can shut down the reactor by covering active catalytic sites. A figure similar to Fig. S1 was assembled describing a region of operation where graphitic and amorphous carbon are not thermodynamically predicted to exist in the solid phase. All points meeting these criteria at adiabatic equilibrium are presented in Figure S2 for $C_{Cellulose}/C_{CH4}=0.25$.

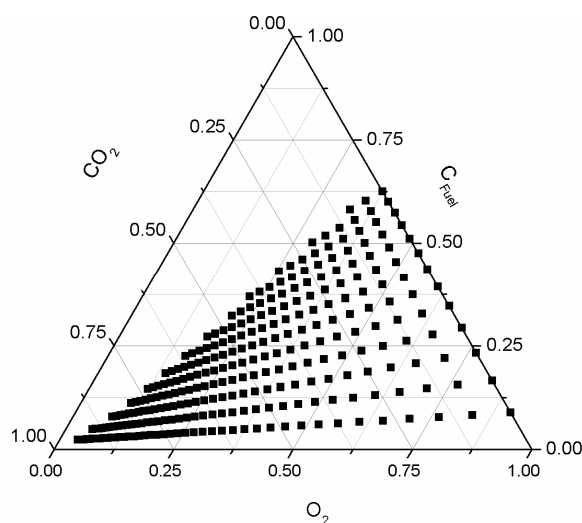**Figure S2:** Adiabatic equilibrium calculations for CPO of cellulose and CH_4 at $C_{Cellulose}/C_{CH4}$=0.25 in air with no preheat and varying ratios of Air/Fuel and Air/CO_2 over all possible concentrations. Results (renormalized without nitrogen) describe a regime where no solid amorphous or graphitic carbon is predicted.

By overlaying Figures S1 and S2, a regime of operation where solid carbon is not a thermodynamic product and there is no net generation of CO_2 in the reactor (Figure S3), corresponding to an area where ≥100% yield of CO is expected.
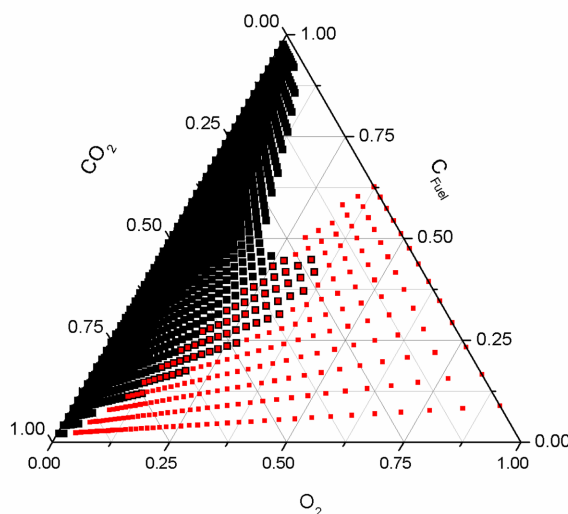

Figure S3: Adiabatic equilibrium calculations for CPO of cellulose and CH_4 at $C_{Cellulose}/C_{CH4}$=0.25 in air with no preheat and varying ratios of Air/Fuel and Air/CO_2 over all possible concentrations. Results (renormalized without nitrogen) overlap to describe a regime of of operation where solid carbon in not a thermodynamic product and there is a net consumption of CO_2 in the reactor, corresponding to an area where >100% yield of CO is expected.

The process described in Figures S1-S3 can be repeated for different $C_{Cellulose}/C_{CH4}$ ratios. Results are presented for four different $C_{Cellulose}/C_{CH4}$ ratios in Figure S4, with the carbon neutral boundaries outlining the areas in which thermodynamic calculations predict zero net generation of CO_2 and no solid carbon formation. Additionally, to give an idea of temperature and fuel to oxygen ratio, selected isotherms and combustion lines were added to the figure based on adiabatic calculations. It should be noted that as the isotherms approach the O_2 axis they do not discontinue. Instead they turn towards the C_{Fuel} axis and continue until intersection. This portion of the isotherms was omitted from the figure for clarity.
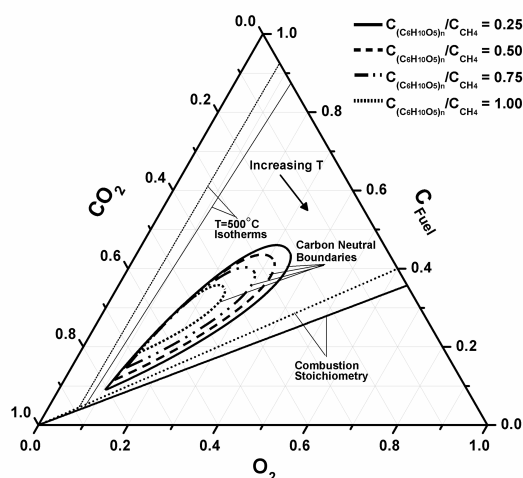
Figure S4: Adiabatic equilibrium calculations for CPO of cellulose and CH_4 at four constant feed ratios in air with no preheat and varying ratios of Air/Fuel and Air/CO_2 over all possible concentrations. Results (renormalized without nitrogen) for each $C_{Cellulose}/C_{CH4}$ ratio outline the areas in which thermodynamic calculations predict zero net generation of CO_2 and no solid carbon formation, corresponding to ≥100% yields of CO.

3) Supporting Information: Construction of Table 1

The construction of Table 1 (also Table S1) required the calculation of a variety of parameters and results. In this section details describing the calculation of C/O ratio, $C_{(C6H10O5)n}/C_{CH4}$, H selectivity to H_2, H selectivity to H_2O, C selectivity to CO, C selectivity to CO_2, C selectivity to CH_4, residence time, mass velocity, H_2/CO, and syngas yield are presented.

Table S1. Selected experimental and theoretical (italics) data for the millisecond CPO of cellulose and CH_4 with CO_2 addition.

Experiment/*Calculation*	1	2	3	4	5	*1*	*2*	*3*	*4*	*5*
Parameters										
Catalyst Bed Length (mm)	60	60	60	60	60	-	-	-	-	-
C/O Ratio	0.6	0.6	0.6	0.6	0.6	*0.82*	*0.79*	*1.00*	*0.91*	*0.70*
$C_{(C6H10O5)n}/C_{CH4}$	∞	5	2	1	0.5	*0.50*	*0.25*	*0.75*	*0.25*	*0.5*
CH_4/O_2 Ratio	0	0.2	0.4	0.6	0.8	*1.09*	*1.27*	*1.14*	*1.45*	*0.93*
CO_2/O_2 Ratio	0	0.91	1.86	2.81	3.76	*1.81*	*1.59*	*0.57*	*0.31*	*2.6*
N_2/O_2 Ratio	3.76	2.86	1.91	0.95	0	*3.76*	*3.76*	*0*	*0*	*0*
Cellulose Flow (g hr^{-1})	50	50	50	50	50	-	-	-	-	-
Results										
Temperature (°C)										
20 mm	1061	1108	1040	1056	1139	-	-	-	-	-
40 mm	1018	965	897	916	985	-	-	-	-	-
Adiabatic	-	-	-	-	-	*652*	*643*	*895*	*892*	*953*
H Selectivity (%)										
H_2	14.9	27.4	26.3	23.7	29.6	*63.9*	*66.4*	*74.9*	*83.6*	*36.6*
H_2O	85.1	72.6	72.9	74.1	68.8	*33.7*	*29.3*	*25.0*	*16.2*	*63.3*
C Selectivity (%)										
CO (Yield*)	19.5	43.0	71.3	94.5	107.6	*100.9*	*101.6*	*101.6*	*101.4*	*131.4*
CO_2	80.5	57.0	28.2	3.9	-8.7	*-2.8*	*-5.4*	*-1.7*	*-1.5*	*-31.4*
CH_4	0	0	0.5	1.6	1.1	*1.8*	*3.7*	*0.0*	*0.1*	*0.0*
Residence Time (ms)	28.1	23.4	19.1	13.7	9.3	-	-	-	-	-
Mass Velocity (hr^{-1})	43.0	51.6	64.5	86.1	129.1	-	-	-	-	-
H_2/CO	0.74	0.55	0.46	0.40	0.41	*1.02*	*1.15*	*1.11*	*1.46*	*0.45*
Syngas Yield (%)	6.5	16.1	27.5	40.0	51.1	*41.6*	*42.8*	*85.1*	*89.6*	*65.1*

* Results for CO selectivity are identical to CO yield because there is always 100% conversion of cellulose to C1 products in the reactor.

The C/O ratio was defined to be:

$$C/O = \frac{\dot{n}_{C,CH_4\ Feed} + \dot{n}_{C,Cellulose\ Feed}}{\dot{n}_{O,O_2\ Feed}} \tag{ES2}$$

where $\dot{n}_{C,CH_4\ Feed}$ is the molar flow rate of carbon in methane in the feed, $\dot{n}_{C,Cellulose\ Feed}$ is the molar flow rate of carbon in cellulose in the feed, and $\dot{n}_{O,O_2\ Feed}$ is the molar flow rate of oxygen in molecular oxygen in the feed.

The ratio of $C_{(C6H10O5)n}/C_{CH4}$ was defined to be:

$$C_{(C_6H_{10}O_5)_n}/C_{CH_4} = \frac{\dot{n}_{C,Cellulose\ Feed}}{\dot{n}_{C,CH_4\ Feed}} \tag{ES3}$$

where $\dot{n}_{C,Cellulose\ Feed}$ is the molar flow rate of carbon in cellulose in the feed and $\dot{n}_{C,CH_4\ Feed}$ is the molar flow rate of carbon in methane in the feed.

The H selectivity to H_2 was defined to be:

$$S_{H_2} = \frac{\dot{n}_{H,H_2\ Effluent}}{\dot{n}_{H,\ Effluent}} \tag{ES4}$$

where $\dot{n}_{H,H_2\ Effluent}$ is the molar flow rate of hydrogen in the molecular hydrogen product stream and $\dot{n}_{H,\ Effluent}$ is the total molar flow rate of hydrogen in the product stream.

The H selectivity to H_2O was defined to be:

$$S_{H_2O} = \frac{\dot{n}_{H,H_2O\ Effluent}}{\dot{n}_{H,\ Effluent}} \tag{ES5}$$

where $\dot{n}_{H,H_2O\ Effluent}$ is the molar flow rate of hydrogen in the water product stream and $\dot{n}_{H,\ Effluent}$ is the total molar flow rate of hydrogen in the product stream.

The C selectivity to CO was defined to be:

$$S_{CO} = \frac{\dot{n}_{C,CO\ Effluent}}{\dot{n}_{C,\ Effluent} - \dot{n}_{C,CO_2\ Feed}} \tag{ES6}$$

where $\dot{n}_{C,CO\ Effluent}$ is the molar flow rate of carbon in the carbon monoxide product stream, $\dot{n}_{C,\ Effluent}$ is the total molar flow rate of carbon in the product stream, and $\dot{n}_{C,CO_2\ Feed}$ is the molar flow rate of carbon in carbon dioxide in the feed. The values for carbon selectivity to CO are identical to CO yield because conversion is always 100% in the reactor system.

The C selectivity to CO_2 was defined to be:

$$S_{CO_2} = \frac{\dot{n}_{C,CO_2\ Effluent} - \dot{n}_{C,CO_2\ Feed}}{\dot{n}_{C,\ Effluent} - \dot{n}_{C,CO_2\ Feed}} \tag{ES7}$$

where $\dot{n}_{C,CO_2\ Effluent}$ is the molar flow rate of carbon in the carbon dioxide product stream, $\dot{n}_{C,CO_2\ Feed}$ is the molar flow rate of carbon in carbon dioxide in the feed, and $\dot{n}_{C,\ Effluent}$ is the total molar flow rate of carbon in the product stream.

The C selectivity to CH_4 was defined to be:

$$S_{CH_4} = \frac{\dot{n}_{C, CH_4\, Effluent}}{\dot{n}_{C,\, Effluent} - \dot{n}_{C, CO_2\, Feed}}$$ (ES8)

where $\dot{n}_{C, CH_4\, Effluent}$ is the molar flow rate of carbon in the methane product stream, $\dot{n}_{C,\, Effluent}$ is the total molar flow rate of cabron in the product stream, and $\dot{n}_{C, CO_2\, Feed}$ is the molar flow rate of carbon in carbon dioxide in the feed.

The residence time was defined to be:

$$RT = \frac{Void\ Space\ in\ Catalyst\ Bed}{Volumetric\ Flow\ Rate\ of\ Effluent\ Gases}$$ (ES9)

Note: Residence times were calculated using the effluent, which contains more moles of gaseous species than the feed. Residence times calculated using the feed varied by no more than 25% from the results presented in Table S1.

The mass velocity was defined to be:

$$MV = \frac{Mass\ Flow\ Rate\ of\ C\ in\ Fuel\ Feed}{Mass\ of\ Catalyst\ (Rh + Ce)}$$ (ES10)

The H_2/CO ratio was defined to be:

$$H_2/CO = \frac{\dot{n}_{H_2,\, Effluent}}{\dot{n}_{CO,\, Effluent}}$$ (ES11)

where $\dot{n}_{H_2,\, Effluent}$ is the molar flow rate of molecular hydrogen in the product stream and $\dot{n}_{CO,\, Effluent}$ is the molar flow rate of carbon monoxide in the product stream.

The syngas yield was defined to be:

$$Syngas\ Yield = \frac{\dot{n}_{CO,\, Effluent} + \dot{n}_{H_2,\, Effluent}}{\dot{n}_{Effluent} - \dot{n}_{CO_2,\, Feed}}$$ (ES12)

where $\dot{n}_{CO,\, Effluent}$ is the molar flow rate of carbon monoxide in the product stream, $\dot{n}_{H_2,\, Effluent}$ is the molar flow rate of molecular hydrogen in the product stream, $\dot{n}_{Effluent}$ is the total molar flow rate of all molecules in the product stream, and $\dot{n}_{CO_2,\, Feed}$ is the molar flow rate of carbon dioxide in the feed.

4) Supporting Information: Comparison of Integrated vs. Independent Reforming

In order to compare theoretical results obtained by independently reforming cellulose and methane with results obtained by the simultaneous co-reforming of both fuels, adiabatic equilibrium calculations were performed using HSC equilibrium solver.[5] Information is presented for four different feed conditions in Table S2.

Parameters used for calculations 1a, 2a, 3a and 4a are for independent cellulose reforming. Parameters used for calculations labelled 1b, 2b, 3b and 4b are for independent methane reforming. Parameters used for calculations 1c, 2c, 3c and 4c are for simultaneous co-reforming of both fuels.

Adiabatic equilibrium temperature results are included for each calculation performed. Adiabatic equilibrium selectivities to H_2, H_2O, CO, CO_2 and the H_2/CO ratio are presented for: 1) the mixed product streams from independent cellulose reforming and independent methane reforming, and 2) the product stream for simultaneous co-reforming of cellulose and methane. Results obtained after mixing products from the independent reforming of each fuel are presented in italics and centred between columns labelled 'a' and 'b' for each of the four feed conditions considered. Results obtained from concurrent reforming of both fuels are presented in regular font in columns 1c, 2c, 3c and 4c. The data demonstrates a substantial improvement in carbon efficiency through co-reforming, rather than independent cellulose and methane reforming followed by mixing.

Table S2. Theoretical data at four different feeds for the reforming of cellulose (a) and methane (b) with mixed product streams (italics), and the co-reforming of cellulose and methane (c), both with carbon dioxide addition

Calculation	1a	1b	1c	2a	2b	2c	3a	3b	3c	4a	4b	4c
Parameters												
C/O Ratio	0.6	0.6	0.6	0.6	0.6	0.6	0.6	0.6	0.6	0.8	0.8	0.8
$C_{(C6H10O5)n}/C_{CH4}$	∞	0	5	∞	0	2	∞	0	1	∞	0	0.5
CO_2/O_2 Ratio	0.91	0.91	0.91	1.86	1.86	1.86	2.81	2.81	2.81	3.76	3.76	3.76
N_2/O_2 Ratio	2.86	2.86	2.86	1.90	1.90	1.90	0.95	0.95	0.95	0.00	0.00	0.00
Results												
Adiabatic Temperature (°C)	1677	960	1536	1565	863	1306	1468	806	1110	1161	617	673
H Selectivity (%)												
H_2	*21.4*		10.6	*28.3*		14.0	*32.0*		18.2	*45.8*		50.8
H_2O	*78.6*		89.4	*71.7*		86.0	*67.9*		81.8	*47.6*		48.4
C Selectivity (%)												
CO (Yield)	***44.4***		**55.7**	***65.4***		**82.9**	***87.9***		**107.5**	***107.1***		**123.9**
CO_2	*55.6*		44.3	*34.6*		17.1	*12.1*		-7.5	*-12.8*		-24.5
H_2/CO	*0.48*		0.19	*0.43*		0.17	*0.36*		0.17	*0.43*		0.41

References
[1] P. J. Dauenhauer, B. J. Dreyer, N. J. Degenstein, L. D. Schmidt, *Angewandte Chemie*. **2007**, *47*, 5864-5867.
[2] J. L. Colby, P. J. Dauenhauer, L. D. Schmidt, *Green Chemistry*. **2008**, *10*, 773-783.
[3] A. S. Bodke, S. S. Bharadwaj, L. D. Schmidt, *Journal of Catalysis*. **1998**, *179*, 138-149.
[4] I. Milosavljevic, V. Oja, E.M. Suuberg, *Ind. Eng. Chem. Res.* **1996**, *35*, 653-662.
[5] Oy, O.R., HSC Chemistry. 2007, Outokupu Research Oy.